Department of Pharmaceutics[1], China Pharmaceutical University[2]; Jiangsu Province Academy of Traditional Chinese Medicine, Nanjing, PR China

Cell uptake of paclitaxel solid lipid nanoparticles modified by cell-penetrating peptides in A549 cells

YIN-LONG ZHANG[1], ZHEN-HAI ZHANG[2], TIAN-YUE JIANG[1], AYMAN-WADDAD[1], JING-LI[1], HUI-XIA LV[1], JIAN-PING ZHOU[1]

Received March 22, 2012, accepted April 30, 2012

Dr. Huixia Lv, Prof. Jianping Zhou, Department of Pharmaceu tical, China Pharmaceutical University, No. 24 Tong jia Xiang, Nan jing 210009, China
lvhxcpu@126.com; zhoujpcpu@126.com

Pharmazie 68: 47–53 (2013) *doi: 10.1691/ph.2013.2071*

The aim of this study was to investigate the cytotoxicity of paclitaxel solid lipid nanoparticles (SLN) modified with stearic acid octaarginine (SA-R_8-PTX-SLN) as well as the cellular uptake of coumarin-6-loaded SLN modified with SA-R_8 (SA-R_8-C_6-SLN) in human lung cancer cells, A549. SLN were prepared using a film dispersion method; and then their particle size, zeta potential, morphology, bound efficiency of SA-R_8, drug loading efficiency, and *in vitro* release were characterized. SA-R_8-PTX-SLN and SA-R_8-C_6-SLN were incubated with A549 cells to measure their cytotoxicity and cellular uptake, respectively. The results indicated that the cytotoxicity of SA-R_8-PTX-SLN was enhanced significantly with the increasing amount of SA-R_8 and the cellular uptakes of SLN increased with the incubated concentrations and the incubated time of SLN. In contrast, SA-R_8-SLN could significantly enhance the cellular uptake of SLN and the cytotoxicity of PTX in A549 cells. These *in vitro* results suggest that SA-R_8-SLN could be proposed as alternative drug delivery system.

1. Introduction

Cell-penetrating peptides (CPPs), also known as protein transduction domains (PTDs), are relatively short peptides consisting of 5 to 40 amino acid residuals with the ability to cross the plasma membrane and enter the cell interior. CPPs can also promote the intracellular delivery of covalently or non-covalently conjugated bioactive cargoes, such as drugs (Aroui et al. 2010a; Aroui et al. 2010b); peptides and siRNA (Endoh and Ohtsuki 2009); proteins and nucleic acids (Deshayes et al. 2008); metal complexes (Rijt et al. 2011); micelles (Sawant and Torchilin 2009); liposomes (Qin et al. 2011); and nanoparticles (Lee et al. 2011). Among CPPs, arginine-rich derivatives of the HIV Tat (RKKRRQRRR) are the most widely studied Tat peptide (Barnes and Shen 2009; Takayama et al. 2009; Walrant et al. 2011; Yang et al. 2008). Interestingly, homopeptides consisting of 7 to 9 arginines display higher cellular uptake compared to the Tat peptide itself (Wender et al. 2000). The addition of fatty acid (FA) to the polyarginines dramatically improves the cellular uptake of polyarginines (Futaki et al. 2001; Katayama et al. 2011; Mae et al. 2009).

Solid lipid nanoparticles (SLN) that consist of a solid phase lipid core surrounded by particle stabilizers are a relatively new class of drug carrier. In recent years, SLN have attracted increased attention because of their favorable features, such as controlled drug release and targeting, protection against chemical degradation, no carrier biotoxicity, and the potential to be scaled up for industrial production (Müller et al. 2000; Wissing et al. 2004). However, there are few studies on the uptake of CPP-modified SLN; thus, in the current work, we developed coumarin-6-loaded SLN and investigated whether or not CPP could enhance the uptake of SLN in A549 cells.

Paclitaxel (PTX), a diterpenoid isolated from the needles and bark of *Taxus brevifolia*, has been used in the treatment of a wide variety of human malignancies, including breast cancer, ovarian cancer, and non-small cell lung cancer (Panchagnula 1998). Numerous studies on SLN as carriers of PTX have been published in recent years (Lee et al. 2007; Li et al. 2011; Wu et al. 2010; Yuan et al. 2008). Nevertheless, the effect of CPP on the cytotoxicity of PTX-loaded SLN *in vitro* on A549 cells has not yet to be reported.

The aim of this study is to evaluate the cellular uptake of SLN with and without stearic acid octaarginines (SA-R_8) as well as the cytotoxic effect of PTX-loaded SLN on the human non-small lung cell cancer cell line, A549. The characterization of SLN, such as particle size, zeta potential, bound efficiency of SA-R_8, drug entrapment efficiency, drug loading (DL) and *in vitro* drug release, have been studied in detail. The effects of CPP in enhancing SLN cellular uptake and cytotoxity of PTX-loaded SLN in A549 cells have also been investigated.

2. Investigations, results and discussion

2.1. DL and bound efficiency of SA-R_8

The amount and the binding efficiency of SA-R_8 attached to the SLN were related to the initial SA-R_8 concentration. As shown in Table 1, the amount of SA-R_8 attached to the SA-R_8-C_6-SLN showed no significant difference from SA-R_8-PTX-SLN with the same SA-R_8 concentration. The absolute amount of SA-R_8 attached to SLN increased with the increased initial input SA-R_8, while RBE decreased with the increased amount of SA-R_8.

Table 1: Absolute amount (AA), relative binding efficiency (RBE) and drug loading (DL) of SA-R_8 attached on the coumarin-6 and PTX-SLN with different initial input SA-R_8. n = 3

Amount of SA-R_8 (mg/mL)	C_6-SLN			PTX-SLN		
	AA (mg/mL)	RBE (%)	DL (%)	AA (mg/mL)	RBE (%)	DL (%)
0.5	0.387 ± 0.003	77.47 ± 0.50	8.83 ± 0.05	0.385 ± 0.009	77.07 ± 1.70	8.59 ± 0.17
1	0.647 ± 0.021	64.67 ± 2.08	13.92 ± 0.38	0.575 ± 0.007	57.53 ± 0.65	12.31 ± 0.12
2	0.843 ± 0.021	42.17 ± 1.04	17.41 ± 0.36	0.818 ± 0.020	40.88 ± 0.98	16.63 ± 0.33

2.2. DL and EE determination

The DL values of coumarin-6 and PTX were about 0.01% and 2.0%, respectively, as shown in Table 2. The EE values of coumarin-6 and PTX were higher than 90%. The addition of SA-R_8 slightly decreased the DL capacity and had no significant effect on the EE of SLN (P>0.05).

2.3. Characterization of SLN

The characteristics of counmarin-6-loaded SLN and PTX-loaded SLN such as zeta potential (ζ), mean particle size and polydispersity index (PDI) are listed in Table 2. Zeta potential is a key factor in evaluating the stability of colloidal dispersion. The repulsion among the nanoparticles with the same type of surface charge provides additional stability. In general, a system could be considered a stable formulation when the absolute value of zeta potential was above 30 mV due to electric repulsion. Most of the absolute values of zeta potential for counmarin-6-loaded SLN and PTX-loaded SLN were lower than 30 mV, suggesting that the SLN obtained in the present study did not have sufficient electrostatic stabilization. However, poloxamer188 or Tween 80 on the surface of SLN could provide additional steric stabilization. The zeta potential of C_6-SLN and PTX-SLN changed from negative to positive after modifying with SA-R_8. Meanwhile, the zeta potential of SLN modified with SA-R_8 was a concomitant increase with the increase of the absolute amount of SA-R_8.

As shown in Table 2, the particle size of counmarin-6-loaded SLN and PTX-loaded SLN ranged from 100 nm to 150 nm, which were preferred to accumulate in tumors due to their enhanced permeability and retention (EPR) effect (Kohane 2007). The particle size of PTX-loaded SLN were higher than that of counmarin-6-loaded SLN with the same lipid matrix, which might be due to the increase in the amounts of solid phase produced by the incorporation of PTX into SLN (Yuan et al. 2008). However, there was no significant change in particle size and PDI of SLN after the SA-R_8 modification.

The AFMs of non-modified and modified SLN are shown in Fig. 1. Both appeared as quasi-spherical shapes. The particle sizes of PTX-SLN and 8 wt% SA-R_8-PTX-SLN were about 200 and 150 nm. These values were larger than those measured by the Zetasizer, which could be explained by the fact that fusion phenomena occurred during the preparation of ATM samples (Su et al. 2011; You et al. 2007). Furthermore, the particle size of SA-R_8-PTX-SLN measured by AFM was smaller than that of PTX-SLN. It might be due to the interaction of SA-R_8 with the SLN, which increased the stability of the nanoparticles and protected them against flattening, here the gel was dried on the mica surface (Gualbert et al. 2003).

2.4. In vitro release studies

Figure 2 illustrates the cumulative release profiles of coumarin-6 and PTX from SLN in pH 7.4 PBS with 0.1% (w/v) Tween 80 in 48 h. Both C_6-SLN and PTX-SLN showed no burst drug release and only 20% and 70% of coumarin-6 and PTX released in 48 h, respectively. PTX was released from SLN in a sustained manner, which could provide a possible continuous action against cancer cells. Meanwhile the release rates of coumarin-6 and PTX from SA-R_8-C_6-SLN and SA-R_8-PTX-SLN were all slower than those of C_6-SLN and PTX-SLN. In addition, the percentages of coumarin-6 and PTX released decreased with the increasing of the amount of SA-R_8.

In order to investigate the release mechanism of SLN, the Higuchi-, zero-, first-, Weibull model, and Korsmeyer-Peppas (K-P) models were applied to simulate all those release profiles, and the coefficient of determination (R^2) was used to assess the "fit" of a model equation (Costa and Sousa Lobo 2001). The coumarin-6 and PTX release data were all fitted to Higuchi equations. The K-P model was developed by Korsmeyer (Korsmeyer et al. 1983) and Peppas (1985) and described by Equation (1)

$$f_t = at^n \quad (1)$$

where "a" was a constant incorporating structural and geometric characteristics of the drug dosage form, "n" is the release exponent that was indicative of the drug release mechanism, and the function of "f_t" is the fractional release of drug. When the n value is between 0.5 and 1.0, the release mechanism is a mass transfer following a non-Fickian model (Costa and Sousa Lobo

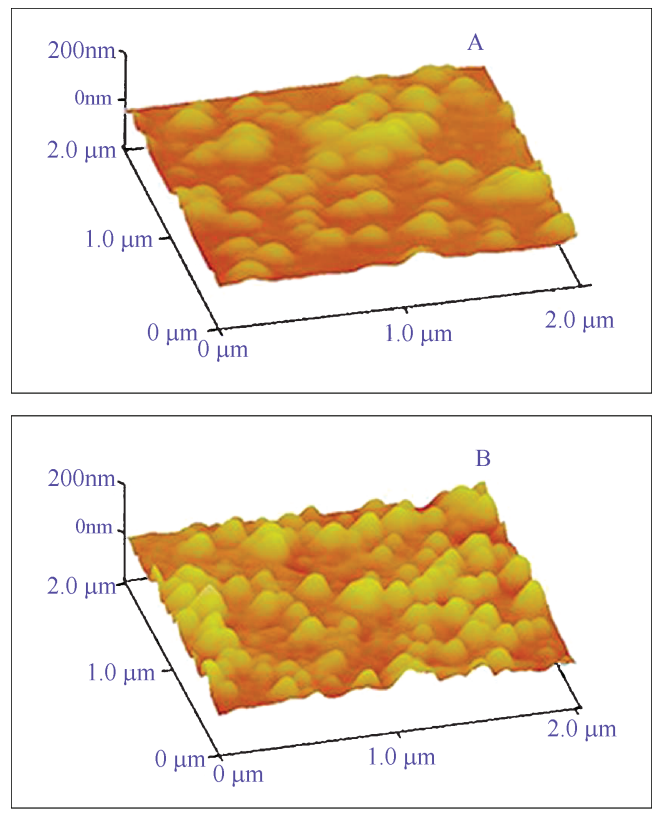

Fig. 1: AFM images of PTX-SLN (A) and 8 wt% SA-R8 modified PTX-SLN (B). (AFM: Atomic force microscopy; PTX: Paclitaxel; SA-R8: Stearic acid modified octaorginine)

Table 2: The characterization of SLN (n = 3)

samples	Size (nm)	PDI	ζ (mV)	EE (%)	DL (%)
C_6-SLN	116.1 ± 6.0	0.247 ± 0.018	−23.0 ± 0.9	92.44 ± 3.28	0.01091 ± 0.00035
CPP_1-C_6-SLN	114.3 ± 6.7	0.236 ± 0.017	18.9 ± 1.3	95.06 ± 2.18	0.01030 ± 0.00021
CPP_2-C_6-SLN	109.2 ± 2.5	0.265 ± 0.005	28.2 ± 2.1	89.89 ± 1.95	0.00808 ± 0.00016
CPP_3-C_6-SLN	107.3 ± 0.6	0.261 ± 0.008	29.3 ± 4.5	94.00 ± 1.60	0.00810 ± 0.00013
PTX-SLN	134.7 ± 1.3	0.298 ± 0.055	−22.0 ± 2.4	97.06 ± 2.02	2.37 ± 0.05
CPP_1-PTX-SLN	135.7 ± 2.9	0.244 ± 0.024	19.4 ± 2.8	93.01 ± 2.60	2.08 ± 0.06
CPP_2-PTX-SLN	131.8 ± 4.9	0.246 ± 0.022	28.3 ± 3.6	92.23 ± 3.40	1.97 ± 0.07
CPP_3-PTX-SLN	129.4 ± 4.8	0.264 ± 0.010	36.3 ± 5.8	93.39 ± 3.50	1.90 ± 0.07

2001). The n values of all release profiles were between 0.8 and 0.9, suggesting that several mechanisms may be involved in the drug release from SLN.

2.5. Cytotoxicity

The cytotoxicity of blank SLN, SA-R_8 modified blank SLN and the mixture of Cremophor EL and ethanol are shown in Fig. 3A. The percentage survival of A549 cells after exposure to SLN and the mixture of Cremophor EL and ethanol decreased significantly with increased concentration of vehicles. The percentage survival of the cells after exposure to the mixture of Cremophor EL and ethanol were 35.77 ± 8.61%, 7.05 ± 1.65% and 2.73 ± 0.70% respectively, at 200 μg/ml, 400 μg/ml and 800 μg/ml. For SLN, at 200 μg/ml, the percentage survival was more than 80%, but at 400 μg/ml, this decreased significantly with the increased amount of SA-R_8 ($P < 0.05$). The percentage survival of cells after exposure to blank SLN as well as blank SLN with 8 wt%, 12 wt% and 16 wt% SA-R_8 were 93.00 ± 10.03%, 31.97 ± 5.98%, 26.09 ± 8.85% and 3.86 ± 0.46%, respectively. At 800 μg/ml, the percentage

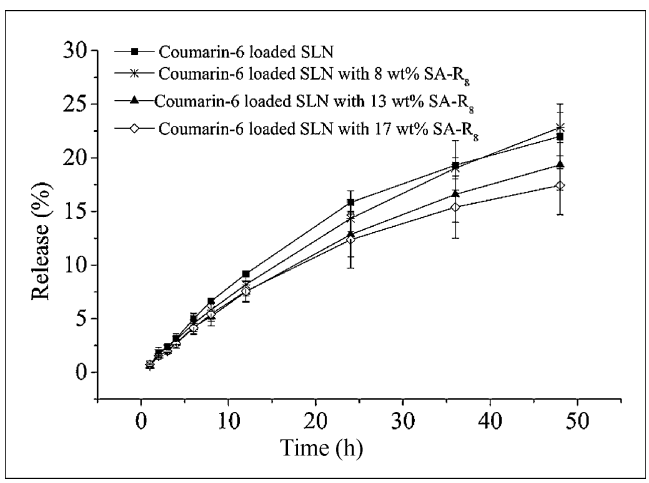

(A)

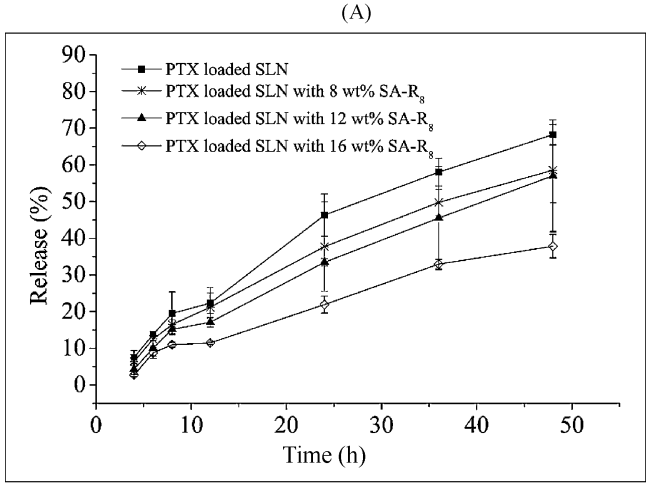

(B)

Fig. 2: *In vitro* drug release curves. (A) Coumarin-6 release from coumarin-6 loaded SLN and coumarin-6 loaded SLN modified with SA-R_8. (B) Paclitaxel (PTX) release from paclitaxel loaded SLN and paclitaxel loaded SLN modified with SA-R_8. n = 3

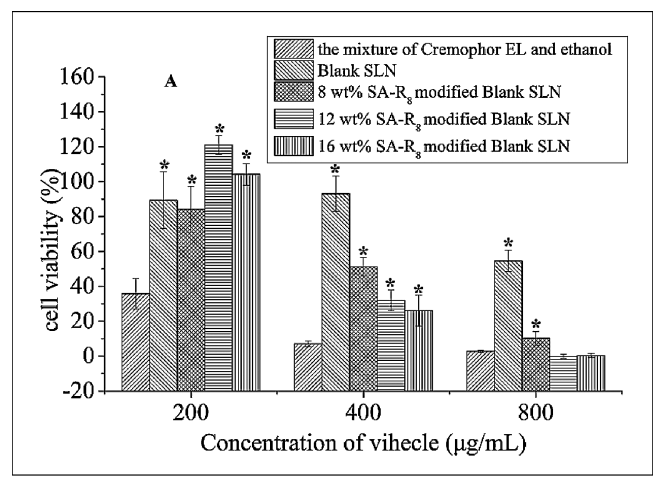

(A)

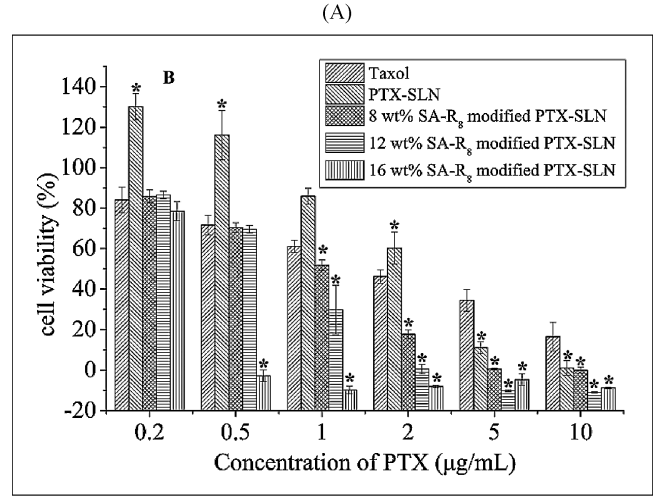

(B)

Fig. 3: Viability of A549 cells. (A) the A549 cells were incubated with blank SLN, SA-R_8 modified blank SLN and the mixture of Cremophor EL and ethanol respectively for 48 h; *: Significantly different from the mixture of Cremophor EL and ethanol at $P < 0.05$. (B) The A549 cells were incubated with PTX solution (Taxol), PTX-SLN, SA-R_8 modified PTX-SLN respectively for 48 h; *: Significantly different from Taxol at $P < 0.05$. (PTX: Paclitaxel; SA-R_8: Stearic acid modified octaorginine; Mean ± S.D., n = 5)

survival of cells after exposure to SLN without SA-R_8 was 54.06 ± 6.04, while exposure to SLN with SA-R_8 showed lower than 10% survival. In contrast, the cytotoxicity of the materials prepared for SLN was significantly lower than that of the mixture of Cremophor EL and ethanol ($P < 0.05$). The results also showed that the materials prepared for SLN without CPP was non-toxic before 400 μg/ml and had a certain cytotoxicity at 800 μg/ml, which was consistent with previous literature (Yuan et al. 2008). The fatty acid-modified octaarginine had no cytotoxicity even at high concentration, but it could promote the uptake of nanoparticles (Katayama et al. 2011), so it was supposed that the SLN uptake increased with the increased amount of SA-R_8, resulting in gradually-enhanced cytotoxicity.

The viability of A549 cells exposed to PTX solution (Taxol), PTX-SLN, and SA-R_8-PTX-SLN after 48 h are shown in Fig. 3B. The cytotoxicity of different formulations of paclitaxel tested showed a dose-dependent manner and the percentage survival of A549 cells after exposure to SA-R_8-PTX-SLN was decreased with the inceasing amount of SA-R_8. The 50% growth inhibition (IC_{50}) values of cells for Taxol, PTX-SLN and SA-R_8-PTX-SLN with 8 wt% and 12 wt% SA-R_8 were 2.133 ± 0.391 μg/ml, 2.551 ± 0.274 μg/ml, 1.139 ± 0.064 μg/ml and 0.806 ± 0.171 μg/ml respectively. In additon, the percentage survival of A549 cells exposed SA-R_8-PTX-SLN with 16 wt% SA-R_8 was about 0% at 0.5 μg/ml, so the IC_{50} could not be calculated. The results showed that the cytotoxicity of Taxol was significantly stronger than that of PTX-SLN ($P < 0.05$), which may be due to the cytotoxicity of the diluent Cremophor EL in Taxol. After PTX-SLN modified with SA-R_8, the cytotoxicity of SA-R_8-PTX-SLN was significantly enhanced versus Taxol and PTX-SLN($P < 0.05$), which could be attributed to the faster cellular uptake of SLN caused by the SA-R_8.

2.6. Cellular uptake of fluorescent SLN

The cellular uptakes of C_6-SLN and 8 wt% SA-R_8-C_6-SLN were evaluated by employing fluorescent microscopy; the measurement of fluorescent intensity was evaluated using a FACS instrument. At first, A549 cells were incubated with different concentrations of SLN for 6 h at 37 °C. Figs. 4A and 5A show the cellular uptakes of SLN with and without SA-R_8 in A549 cells against the incubated concentrations. The cellular uptakes of SLN increased with the incubated concentrations of SLN at the same incubation time, and the cellular uptakes of SA-R_8-C_6-SLN were higher than those of SLN without SA-R_8 in A549 cells ($P < 0.05$).

In order to study the time course of SLN uptake by cells, A549 cells were incubated with 90 μg/ml C_6-SLN for 1 h, 3 h, 6 h, 12 h, and 24 h at 37 °C. Fig. 4B showed that the fluorescent intensity of the cell cytoplasm enhanced as the incubation time increased from 1 h to 24 h. A similar trend of SLN uptake by A549 cells was observed by FACS analysis (Fig. 5B). Those suggested that particle uptake of SLN was a time-dependent process. SA-R_8-C_6-SLN enhanced the cell uptake compared to the C_6-SLN. The results also showed that the uptake of SA-R_8-C_6-SLN at any time was always significantly higher than that of C_6-SLN ($P < 0.05$). This was consistent with previous studies (Furukawa et al. 2011).

The effect of incubation temperature on the cellular uptake of SLN was studied for A549 cells. The uptakes of 90 μg/ml SLN by cells at 4 °C and 37 °C were visualized using fluorescent microscopy. From Fig. 4C, it is evident that the fluorescence intensity of cells incubated with SLN at 37 °C was higher than that of cells incubated with SLN at 4 °C. To evaluate quantitatively the effect of incubation temperature on the cellular uptake of SLN, fluorescence intensity was measured by FACS (Fig. 5C). At 4 °C, the fluorescence intensity of cells incubated by the C_6-SLN and SA-R_8-C_6-SLN (8 wt%) decreased by 19.78 ± 11.40% and 31.11 ± 14.84, respectively, compared with cells incubated with SLN at 37 °C, indicating that the obtained SA-R_8-SLN appeared to enter the cell via energy-dependent transport (Maiolo et al. 2005).

3. Experimental

3.1. Materials

PTX was purchased from Shanghai Sunve Pharmaceutical Co., Ltd (Shanghai, China), while SA-R_8 was purchased from Shanghai Gil Chemical Co., Ltd (Shanghai, China). Soybean phospholipid was obtained from Shanghai Taiwei Pharmaceutical Co., Ltd (Shanghai, China). Monostearin, poloxamer188 and Tween 80 were purchased from Shanghai Chemical Reagent Co., Ltd (Shanghai, China). 3-(4,5-dimethylthiazol-2-yl)-2,5-diphenyl-tetrazolium bromide (MTT) and coumarin-6 were obtained from Sigma (St. Louis, MO, USA). Trypsin and RPMI Medium 1640 were purchased from GibcoBRL (Gaithersberg, MD, USA). All other solvents were of analytical or chromatographic grades.

3.2. Cell culture

A549 cells were cultured in RPMI1640 with 10% FBS and antibiotics, at 37 °C in a humidified atmosphere containing 5% CO_2. These were subcultured every 2 days with 0.25% trypsin.

3.3. SLN preparation

The PTX-loaded SLN were prepared using a modified film dispersion method (Lu et al. 2006). Lipid matrix containing monostearin and soybean phospholipid fixed at a mass ratio of 1:1 (w/w) and PTX (2.5 wt % of lipid matrix) were dissolved in the chloroform (3 ml) at a 100 ml round-bottomed flask. The organic solvent was vacuum-evaporated in a rotary evaporator at 30 °C with 30 rpm for 1 h to form the lipid film. The lipid film was dried overnight through evacuation in desiccators under reduced pressure. A solution containing 0.1 wt% poloxamer188 and 0.1wt % Tween 80 was added under mechanical agitation (DC-40; Hangzhou Electrical Engineering Instruments, China) until homogeneous crude emulsions were formed. These emulsions were ultrasonicated by using a microtip probe sonicator (Beidi-YJ, Nanjing Beidi Laboratory Apparatus Co., Ltd., China) at pulse on 1.0 second and pulse off 1.0 second. This was done at 25% amplitude for 30 min to form SLN dispersion. The untrapped drug was removed by filtration through a 0.22 μm cellulose nitrate filter membrane. Coumarin-6-loaded SLN was prepared with coumarin-6 (C_6, 50 μg) instead of PTX.

CPP-modified SLN were prepared using the incubation method (Homhuan et al. 2009). SA-R_8, with 12.5 wt %, 25 wt%, and 50 wt % of lipid matrix respectively, were added into SLN dispersion under mechanical agitation at 4 °C for 12 h. The non-modified and modified SLN loaded with coumarin-6 and PTX were named as C_6-SLN, CPP_1-C_6-SLN, CPP_2-C_6-SLN, CPP_3-C_6-SLN, PTX-SLN, CPP_1-PTX-SLN, CPP_2-PTX-SLN, and CPP_3-PTX-SLN, respectively.

3.4. DL and bound efficiency of SA-R_8

Aliquots of SA-R_8-modified SLN dispersion (0.1 ml) were centrifuged at 10,000 rpm for 10 min in an ultimate filtration tube (molecular weight cut 10,000). The SLN pellet was then re-suspended with 0.1 ml distilled water and was centrifuged (TGL-16C; Shanghai Anting Science Instruments, China) twice. The non-bound SA-R_8 in the bottom of the tube was determined by HPLC by using an LC-10Avp Shimadzu pump and LC-10Avp Shimadzu UV-VIS detector. A mixture of acetonitrile and water (51:49, v/v) was used as the mobile phase. The chromatographic conditions employed were as follows: Shim-pack CLC-ODS column with temperature at 30 °C (5 μm, 150 mm, 6 mm i.d), flow rate of 1.0 ml/min, detection at 220 nm and sample injected volume of 20 μl. The calibration curve for the quantification of SA-R_8 was linear over a range of standard concentrations of SA-R_8 from 10 $\mu g.ml^{-1}$ to 200 $\mu g.ml^{-1}$, with a correlation coefficient $R^2 = 0.9997$. The limit of detection was 10 $\mu g.ml^{-1}$. The relative binding efficiency (RBE) and DL of SA-R_8 attached to the SLN were calculated using Eq. (2) and (3), respectively:

$$RBE(\%) = (W_{total} - W_{filtered})/W_{total} * 100\% \quad (2)$$

$$DL(\%) = (W_{total} - W_{filtered})/(W_{total} - W_{filtered} + W_L) * 100\% \quad (3)$$

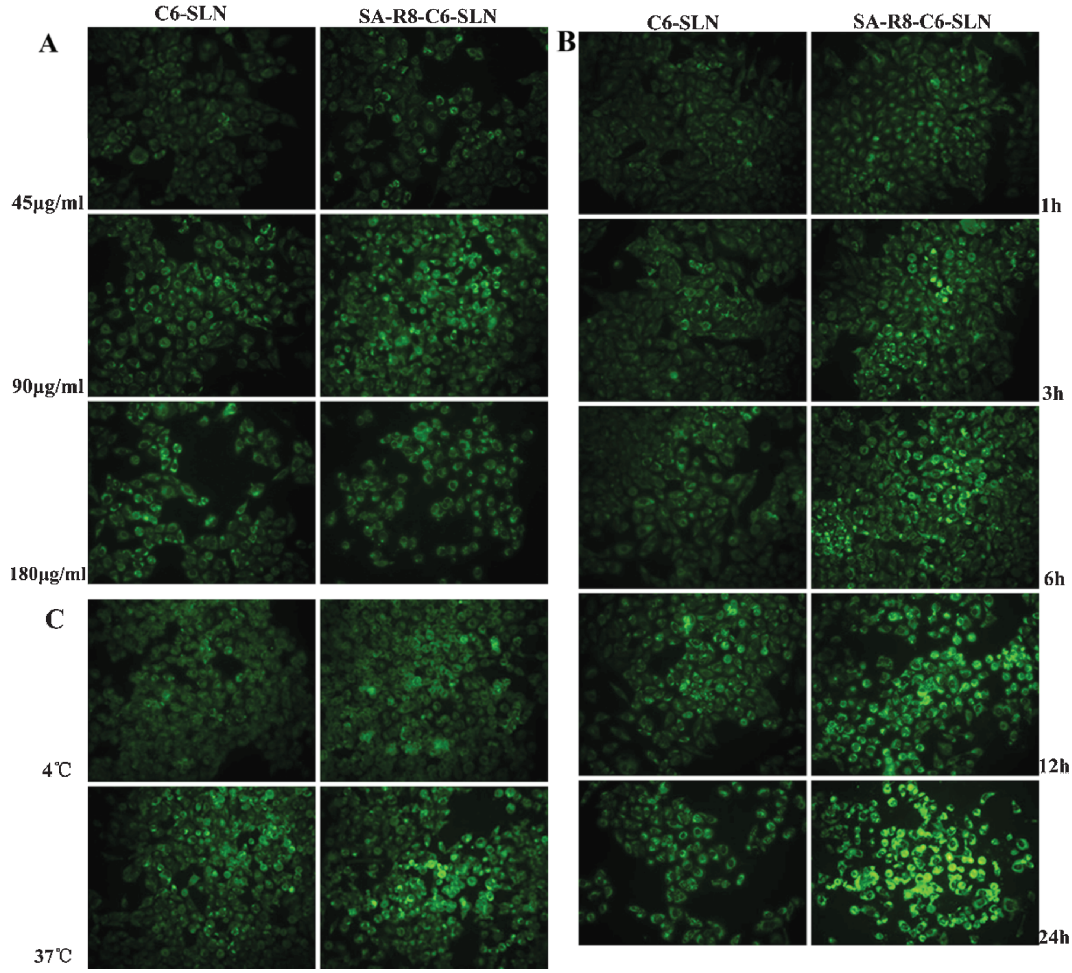

Fig. 4: Fluorescence images after the A549 cells were incubated with C_6-SLN and SA-R_8-C_6-SLN. (A) The A549 cells were incubated with different concentrations of SLN for 6 h at 37 °C. (B) The A549 cells were incubated with 90 μg/ml of SLN for different time at 37 °C. (C) The A549 cells were incubated with 90 μg/ml of SLN for 6h at 37 °C and 4 °C. (C_6: Coumarin-6; SA-R_8: Stearic acid modified octaorginine; SA-R_8-C_6-SLN: C_6-SLN modified with 8 wt% SA-R_8)

where W_{total} is the weight of SA-R_8 added in SLN, $W_{filtered}$ is the weight of SA-R_8 analyzed after filtration, and W_L is the weight of lipid matrix added in system.

3.5. Characterizations of SLN

The mean particle size and the zeta potential of the SA-R_8-PTX-SLN and SA-R_8-C_6-SLN diluted 20 times with distilled water were determined with Zetasizer (3000HS, Malvern Instruments, UK). SLN morphology was characterized by atomic force microscopy (AFM) (Veeco diNanoScope V, USA). Before observation, one drop of properly-diluted SLN dispersion was placed on the surface of a clean silicon wafer, and dried overnight at room temperature. Then the sample was observed by the AFM with a 5 μm scanner in contact mode.

3.6. DL capacity and entrapment efficiency (EE) determination

The EE of PTX was determined by the amount of PTX in SLN after filtration as previously described (Castro et al. 2009, 2007). Briefly, an aliquot of the SLN dispersion was dissolved in methanol. The supernatant after centrifugation (10,000 rpm for 10 min) was measured by HPLC using an LC-10Avp Shimadzu pump and LC-10Avp Shimadzu UV-VIS detector. A mixture of methanol and water (75:25, v/v) was used as the mobile phase. The chromatographic conditions employed were as follows: Lichrospher C_{18} column with temperature at 30 °C (5 μm, 250 mm, 4.6 mm i.d), flow rate of 1.0 ml/min, detection at 227 nm, and injected sample volume of 20 μl. The calibration curve for the quantification of PTX was linear over a range of standard concentrations of PTX from 0.1 μg.ml $^{-1}$ to 50 μg.ml $^{-1}$, with a correlation coefficient R^2 = 0.9999. The limit of detection was 0.1 μg.ml^{-1}.

Coumarin-6 loading capacity and EE of coumarin-6-loaded SLN were measured by HPLC using an LC-10Avp Shimadzu pump and LC-10Avp Shimadzu fluorescence detector set at Ex465 nm/Em503 nm. A mixture of methanol and 2 mM ammonium acetate buffer (95:5, pH4.0) was used as the mobile phase. The calibration curve for the quantification of coumarin-6 was linear over a range of standard concentrations from 0.05 ng.ml $^{-1}$ to 20 ng.ml $^{-1}$, with a correlation coefficient R^2 = 0.9996. The limit of detection was 0.05 ng.ml^{-1}. The sample preparation and other chromatographic conditions were the same as the method of DL and EE determination for PTX.

The drug (coumarin-6 or PTX) EE and DL of SLN were calculated from Eq. (4) and (5), respectively:

$$RBE\% = W_{filtered}/W_{total} * 100\% \quad (4)$$

$$DL(\%) = W_{filtered}/(W_{filtered} + W_L) * 100\% \quad (5)$$

where W_{total} is the weight of drug added in SLN, $W_{filtered}$ is the weight of drug analyzed after filtration, and W_L is the weight of lipid matrix added in system.

3.7. In vitro release studies

The *in vitro* release of coumarin-6 or PTX from SLN was investigated using the membrane dialysis method. The SLN suspension in dialysis bags (7,000 Da molecular weight cut-off) was dialyzed in pH 7.4 phosphate buffered saline (PBS) with 0.1% (w/v) Tween 80. Meanwhile, coumarin-6 or PTX methanol solution was prepared as the control specimen. The temperature and speed of the shaker were maintained at 37 °C and 100 rpm, respectively. The experiments were carried out for 48 h in triplicate. At predetermined time intervals, samples (1 ml) were withdrawn and replaced with equivalent fresh medium. The samples were centrifuged at 10,000 rpm for 10 min, and the supernatant was determined by HPLC method as described above.

3.8. SLN cytotoxicity

Cellular cytotoxicity was determined by an MTT dye reduction assay as previously reported (Krieger et al. 2010; Ulbrich et al. 2011). A549 cells (1×10^4/well) were seeded in a 96-well plate and cultured for 24 h. The growth medium was removed, after which paclitaxel solution (Taxol), PTX-SLN, SA-R_8-PTX-SLN and blank SLN, the mixture of Cremophor EL and

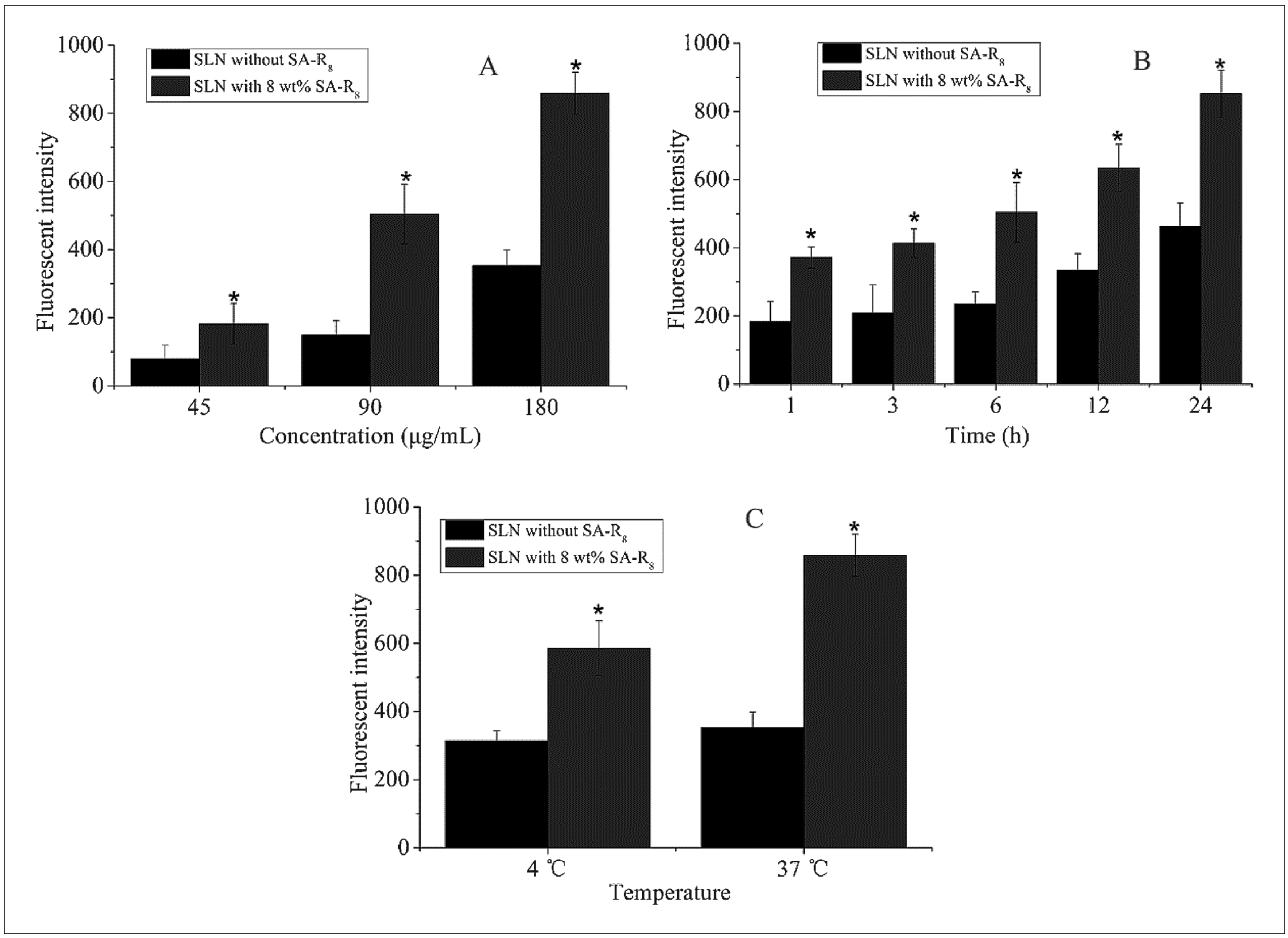

Fig. 5: FACS analysis of the cellular uptakes of fluorescent SLN in A549 cells. (A) The cellular uptakes after the A549 cells were incubated with different concentrations of SLN for 6 h at 37 °C. (B) The cellular uptakes after the A549 cells were incubated with 90 μg/ml SLN for different time at 37 °C. (C) The cellular uptakes after the A549 cells were incubated with 180 μg/mL SLN for 6 h at 37 °C and 4 °C. (*: Significantly different from the SLN without SA-R_8 at $P < 0.05$; FACS: The fluorescence-activated cell sorters; SA-R_8: Stearic acid modified octaorginine; Mean ± S.D., n = 3)

ethanol with different concentrations in RPMI 1640 without FBS were added and then incubated for 48 h. MTT (20 μl) PBS solution (5 mg/ml) was added into each well, and cells were further incubated for 4 h. Formazan crystals resulting from the MTT reduction were dissolved by adding 200 μl DMSO after removing the unreduced MTT and medium. Finally, the plates were shaken for 10 min, and the absorbance of formazan product was measured at 570 nm using a microplate reader (BioRad, Model 680, USA). The percentage of cell survival was defined as the relative absorbance of treated cells versus respective controls. All the experiments were performed in triplicate.

3.9. Cellular uptake of SLN

Fluorescent microscopy was used to investigate the qualitative uptake of the SA-R_8-C_6-SLN and the coumarin-6-loaded SLN without SA-R_8(C_6-SLN) by A549 cells. A549 cells (1×10^5/well) in the growth medium were seeded in a 24-well plate and cultured for 24 h. The growth medium was removed, after which SLN with different concentrations (45, 90 and 180 μL/ml, respectively) in RPMI1640 without FBS were added and incubated for different time periods and temperatures. The cells were then washed thrice with PBS 7.4 and fixed by 4% para-formaldehyde in PBS (pH 7.4) at room temperature for 30 min. Cells were washed thrice with PBS 7.4 and then observed under fluorescent microscopy (Nikon, Tokyo, Japan).

The fluorescence-activated cell sorters (FACS) instrument (BD Biosciences, Germany) was used to investigate quantitatively the uptake of the SA-R_8-C_6-SLN and the C_6-SLN by A549 cells. A549 cells (2×10^5/well) in the growth medium were seeded in a 6-well plate and cultured for 48 h. The growth medium was removed, after which the SA-R_8-C_6-SLN and the C_6-SLN with different lipid concentrations (45, 90 and 180 μl/ml, respectively) in RPMI1640 without FBS were added and incubated for different time periods and temperatures. The cells were then washed twice with PBS and incubated with 0.25% trypsin in PBS for 1 min at 37 °C. The cells were harvested and centrifuged at 1,000 rpm for 5 min. The cell pellet was then suspended with 2 ml PBS followed by centrifugation. After an additional two washes with PBS and centrifugation, the cells were suspended in 400 μl of PBS and analyzed by a FACS instrument using 488 nm laser excitation and a 515–545 nm emission filter. Each sample was analyzed for 10, 000 events.

3.10. Statistical analysis

Data were expressed as means of three separate experiments and were compared by analysis of variance (ANOVA). P-value < 0.05 was considered as statistically significant in all cases.

Acknowledgments: This work was supported by the project of research and innovation plans of graduate students in Jiangsu province (CX10B-373Z) and the project of the National Natural Sciences Foundation of China (30973649).

References

Aroui S, Brahim S, Waard MD, Kenani A (2010a) Cytotoxicity, intracellular distribution and uptake of doxorubicin and doxorubicin coupled to cell-penetrating peptides in different cell lines: a comparative study. Biochem Biophys Res Commun 391: 419–425.

Aroui S, Mili D, Brahim S, De Waard M, Kenani A (2010b) Doxorubicin coupled to penetratin promotes apoptosis in CHO cells by a mechanism involving c-Jun NH2-terminal kinase. Biochem Biophys Res Commun 396: 908–914.

Barnes MP, Shen WC (2009) Disulfide and thioether linked cytochrome c-oligoarginine conjugates in HeLa cells. Int J Pharm 369: 79–84.

Castro GA, Coelho ALLR, Oliveira CA, Mahecha GAB, Oréfice RL, Ferreira LAM (2009) Formation of ion pairing as an alternative to improve encapsulation and stability and to reduce skin irritation of retinoic acid loaded in solid lipid nanoparticles. Int J Pharm 381: 77–83.

Castro GA, Orefice RL, Vilela JM, Andrade MS, Ferreira LA (2007) Development of a new solid lipid nanoparticle formulation containing retinoic acid for topical treatment of acne. J Microencapsul 24: 395–407.

Costa P, Sousa Lobo JM (2001) Modeling and comparison of dissolution profiles. Eur J Pharm Sci 13: 123–133.

Deshayes S, Morris M, Heitz F, Divita G (2008) Delivery of proteins and nucleic acids using a non-covalent peptide-based strategy. Adv Drug Deliv Rev 60: 537–547.

Endoh T, Ohtsuki T (2009). Cellular siRNA delivery using cell-penetrating peptides modified for endosomal escape. Adv Drug Deliv Rev 61: 704–709.

Furukawa R, Yamada Y, Takenaga M, Igarashi R, Harashima H (2011) Octaarginine-modified liposomes enhance the anti-oxidant effect of Lecithinized superoxide dismutase by increasing its cellular uptake. Biochem Biophys Res Commun 404: 796–801.

Futaki S, Ohashi W, Suzuki T, Niwa M, Tanaka S, Ueda K, Harashima H, Sugiura Y (2001) Stearylated arginine-rich peptides: a new class of transfection systems. Bioconjug Chem 12: 1005–1011.

Gualbert J, Shahgaldian P, Coleman AW (2003) Interactions of amphiphilic calix[4]arene-based Solid Lipid Nanoparticles with bovine serum albumin. Int J Pharm 257: 69–73.

Homhuan A, Kogure K, Nakamura T, Shastri N, Harashima H (2009) Enhanced antigen presentation and CTL activity by transduction of mature rather than immature dendritic cells with octaarginine-modified liposomes. J Control Release 136: 79–85.

Katayama S, Hirose H, Takayama K, Nakase I, Futaki S (2011). Acylation of octaarginine: Implication to the use of intracellular delivery vectors. J Control Release 149: 29–35.

Kohane DS (2007) Microparticles and nanoparticles for drug delivery. Biotechnol Bioeng 96: 203–209.

Korsmeyer RW, Gurny R, Doelker E, Buri P, Peppas NA (1983) Mechanisms of solute release from porous hydrophilic polymers. Int J Pharm 15: 25–35.

Krieger ML, Eckstein N, Schneider V, Koch M, Royer HD, Jaehde U, Bendas G (2010) Overcoming cisplatin resistance of ovarian cancer cells by targeted liposomes *in vitro*. Int J Pharm 389: 10–17.

Lee JY, Bae KH, Kim JS, Nam YS, Park TG (2011) Intracellular delivery of paclitaxel using oil-free, shell cross-linked HSA–multi-armed PEG nanocapsules. Biomaterials 32: 8635–8644.

Lee MK, Lim SJ, Kim CK (2007) Preparation, characterization and *in vitro* cytotoxicity of paclitaxel-loaded sterically stabilized solid lipid nanoparticles. Biomaterials 28: 2137–2146.

Li R, Eun JS, Lee MK (2011) Pharmacokinetics and biodistribution of paclitaxel loaded in pegylated solid lipid nanoparticles after intravenous administration. Arch Pharm Res 34: 331–337.

Lu.B, Xiong SB, Yang H, Yin XD, Chao RB (2006) Solid lipid nanoparticles of mitoxantrone for local injection against breast cancer and its lymph node metastases. Eur J Pharm Sci 28: 86–95.

Müller RH, Mäder K, Gohla S (2000) Solid lipid nanoparticles (SLN) for controlled drug delivery-a review of the state of the art. Eur J Pharm Biopharm 50: 161–177.

Mae M, El Andaloussi S, Lundin P, Oskolkov N, Johansson HJ, Guterstam P, Langel U. (2009) A stearylated CPP for delivery of splice correcting oligonucleotides using a non-covalent co-incubation strategy. J Control Release 134: 221–227.

Maiolo JR, Ferrer M, Ottinger EA (2005) Effects of cargo molecules on the cellular uptake of arginine-rich cell-penetrating peptides. Biochim Biophys Acta 1712: 161–172.

Panchagnula R (1998) Pharmaceutical aspects of paclitaxel. Int J Pharm 172: 1–15.

Peppas NA (1985) Analysis of Fickian and non-Fickian drug release from polymers. Pharm Acta Helv 60: 110–111.

Qin Y, Chen H, Yuan W, Kuai R, Zhang Q, Xie F, Zhang L, Zhang Z, Liu J, He Q (2011) Liposome formulated with TAT-modified cholesterol for enhancing the brain delivery. Int J Pharm 419: 85–95.

Rijt SH, Kostrhunova H, Brabec V, Sadler PJ (2011) Functionalization of osmium arene anticancer complexes with (poly)arginine: effect on cellular uptake, internalization, and cytotoxicity. Bioconjug Chem 22: 218–226.

Sawant RR, Torchilin VP (2009) Enhanced cytotoxicity of TATp-bearing paclitaxel-loaded micelles *in vitro* and in vivo. Int J Pharm 374: 114–118.

Su Z, Niu J, Xiao Y, Ping Q, Sun M, Huang A, You W, Sang X, Yuan D (2011) Effect of octreotide-polyethylene glycol(100) monostearate modification on the pharmacokinetics and cellular uptake of nanostructured lipid carrier loaded with hydroxycamptothecine. Mol Pharm 8: 1641–1651.

Takayama K, Tadokoro A, Pujals S, Nakase I, Giralt E, Futaki S (2009) Novel system to achieve one-pot modification of cargo molecules with oligoarginine vectors for intracellular delivery. Bioconjug Chem 20: 249–257.

Ulbrich K, Michaelis M, Rothweiler F, Knobloch T, Sithisarn P, Cinatl J, Kreuter J (2011) Interaction of folate-conjugated human serum albumin (HSA) nanoparticles with tumour cells. Int J Pharm 406: 128–134.

Walrant A, Correia I, Jiao CY, Lequin O, Bent EH, Goasdoue N, Lacombe C, Chassaing G, Sagan S, Alves ID (2011) Different membrane behaviour and cellular uptake of three basic arginine-rich peptides. Biochim Biophys Acta 1808: 382–393.

Wender PA, Mitchell DJ, Pattabiraman K, Pelkey ET, Steinman L, Rothbard JB (2000) The design, synthesis, and evaluation of molecules that enable or enhance cellular uptake: peptoid molecular transporters. Proc Nat Acad Sci 97: 13003.

Wissing S, Kayser O, Muller R (2004) Solid lipid nanoparticles for parenteral drug delivery. Adv Drug Deliv Rev 56: 1257–1272.

Wu L, Tang C, Yin C (2010) Folate-mediated solid-liquid lipid nanoparticles for paclitaxel-coated poly(ethylene glycol). Drug Dev Ind Pharm 36: 439–448.

Yang SR, Kim SB, Joe CO, Kim JD (2008) Intracellular delivery enhancement of poly(amino acid) drug carriers by oligoarginine conjugation. J Biomed Mater Res A 86: 137–148.

You J, Wan F, de Cui F, Sun Y, Du YZ, Hu FQ (2007) Preparation and characteristic of vinorelbine bitartrate-loaded solid lipid nanoparticles. Int J Pharm 343: 270–276.

Yuan H, Miao J, Du YZ, You J, Hu FQ, Zeng S (2008) Cellular uptake of solid lipid nanoparticles and cytotoxicity of encapsulated paclitaxel in A549 cancer cells. Int J Pharm 348: 137–145.